

1 in climate models. Better quantification of the radiative forcing by different types of aerosol is
2 needed to improve predictions of future climate (Brock et al., 2011).

3 During the last century the temperature increase in the Arctic has been observed to be
4 larger than the global average (IPCC, 2013). The reason for this “Arctic amplification” relates
5 to both the complex feedbacks that are active in the Arctic environment as well as the overall
6 environmental conditions that are characteristic of the Arctic environment (Quinn et al.,
7 2007). This increased warming results in positive feedback which further impacts the
8 radiative balance via reduced surface albedo (Hudson, 2011). Future changes in the Arctic are
9 projected to progress rapidly and the projections show that the Arctic Ocean may be
10 seasonally ice free in the next several decades. This will result in a more pronounced impact
11 on atmospheric aerosol sources and sinks and on cloud properties and their distribution in the
12 area (Petelski and Piskozub, 2006).

13 Methods commonly used for monitoring atmospheric pollution (including aerosols)
14 are optical ones, which collect data from a given point or a small area (Labow, 1996; Dixon,
15 1998; Drollette, 2000; Smirnov et al., 2002). Studies using ground-based sunphotometry are
16 very effective in investigations of aerosol optical properties. Aerosol optical depth measured
17 at different wavelengths is one of the key parameters in aerosol studies (Dubovik et al., 2002;
18 Zielinski, 2004; Markowicz et al., 2008; Mazzola et al., 2012; Zielinski et al., 2012). Also
19 satellite remote sensing is a good approach to obtain the aerosol information over the Arctic
20 region, for which appropriate aerosol models are required.

21
22 In this paper we describe the aerosol optical depth and Ångström exponent values
23 measured at three locations in Spitsbergen. These stations include Hornsund in the south of
24 the island, Longyearbyen in the center of the island and Ny-Alesund, in the north.

26 **2. Site characteristics and instrumentation**

28 2.1. Station characteristics

29
30 The climate of Svalbard is dominated mostly by its northerly location, while the
31 Norwegian Current and West Spitsbergen Current (which are a continuation of the North
32 Atlantic Current) moderate its temperatures. The Arctic climate is the place where cold polar
33 air from the north and west (high pressure over Greenland and the Polar basin) meets mild,
34 wet sea air from the south (low pressure between Greenland and Spitsbergen) (Treffeisen et
35 al., 2011; Rozwadowska et al., 2010). As a result very active cyclonic circulation (and fronts
36 with cloudy conditions, rain and strong winds are often reported in this region. These are
37 major factors which determine the changeable weather over Svalbard, which in various parts
38 of the archipelago is significantly different. The western part is warmer, while the interior has
39 relatively more continental climate than the coasts.

40 Three sites in Spitsbergen are taken into consideration and they include all available
41 AERONET (AERosol RObotic NETwork) data over Svalbard (<http://aeronet.gsfc.nasa.gov/>).
42 These include stations in Hornsund (77°00'03" N, 15°33'36"E, at 10 m a.s.l.), Longyearbyen
43 (78°13'12"N, 15°38'56"E, at 30 m a.s.l.) and Ny-Alesund (78°55'44"N, 11°51'39"E, at 46 m
44 a.s.l.) (Figure 1).

45 Ny-Alesund is the highest above sea level and most northerly situated station located
46 on Brøggerhalvøya and Kongsfjorden. The village is surrounded by mountains and tundra
47 system. The Svalbard capital town of Longyearbyen – in the middle part of the island, is
48 situated in the valley of Longyeardalen and on the shore of Adventfjorden. Hornsund is the
49 southernmost fjord of the western side of Spitsbergen. The location of the stations has
50 significant impact on the differentiation of air masses moving to the study area.

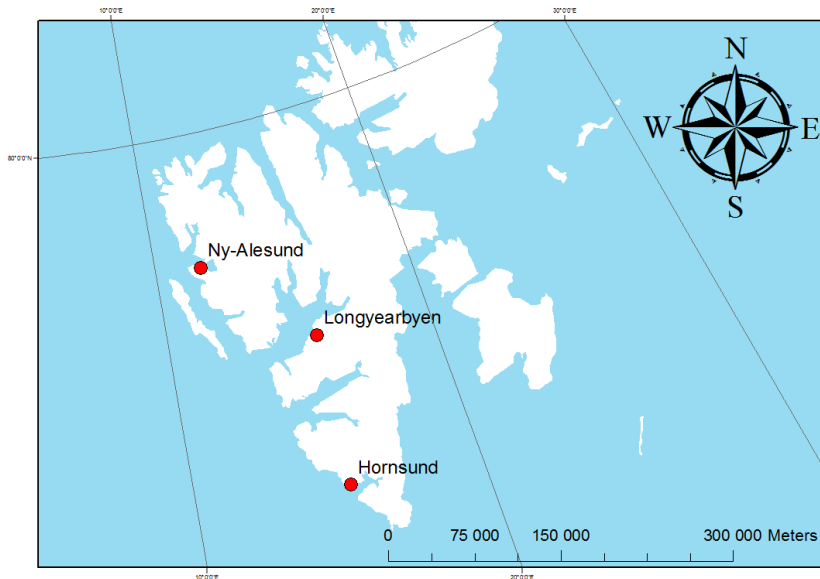


Figure 1. Location of the research stations in Spitsbergen.

1 The AERONET network provides long-term, globally distributed observations of
 2 spectral aerosol optical depth (AOD) as well as Ångström exponent (AE). Ground-based
 3 remote sensing techniques are used to obtain long-term and continuous characterization of
 4 aerosols over the whole world.

5 In Ny-Alesund observations have also been performed in the AWIPEV (French-
 6 German Arctic Research Base at Koldeway station, Ny-Alesund) (<http://www.awipev.eu/>)
 7 (Herber et al., 2002). Since 2001 the Institute of Oceanology Polish Academy of Sciences
 8 (IOPAN) has performed their aerosol studies in the same area as the AERONET, i.e. in
 9 Longyearbyen, Hornsund and Ny-Alesund.

10 2.2. Instruments and database characteristics

11 The database used in this paper is composed of measurements performed in three
 12 different areas of Spitsbergen (Hornsund, Longyearbyen, Ny-Alesund) and different sun
 13 photometers as well as for different time intervals. The instrument and data information are
 14 provided in Table 1 below.

15 Table 1. Instruments and information on data availability.

| No. | Site/Station | Instrument | Reference | Data availability | Number of measurement days |
|-----|--------------|--------------|-----------|-------------------|----------------------------|
| 1 | Hornsund | Cimel CE-318 | AERONET | 2005-2012 | 435 |
| | | M-II | IOPAN | 2009-2012 | 9 |
| 2 | Longyearbyen | Cimel CE-318 | AERONET | 2003-2004 | 78 |
| 3 | Ny-Alesund | Cimel CE-318 | AERONET | 2006 | 9 |
| | Ny-Alesund, | SP1A | AWIPEV | 2000-2011 | 594 |
| | Ny-Alesund | M-II | IOPAN | 2001-2012 | 13 |

1
2 For all locations we use data from a period of March 2000 to September 2012. At the
3 Svalbard latitude sunphotometric measurements cannot be performed all year round due to the
4 polar night. At these latitudes the sun does not rise between late September and early March.
5 We accepted the approach that when sun is over the horizon for a period shorter than 10 hours
6 per day and during the polar night we have winter and autumn. Summer is defined for days
7 when sun occurs for an entire day while, spring - for more than 10 hours a day and only for
8 measurements which were carried out before the defined summer. Such an approach resulted
9 in a reduced number of data. We use data from only spring and summer months. Secondly,
10 only clear sky conditions enable to make any solar measurements and thus the number of
11 “good” measurement days is also limited.

12 The AERONET protocols impose standardization of instruments, data quality,
13 processing and calibration (Holben et al., 1998). The measurements are acquired with Cimel
14 sun photometer CE-318. This automatic sun and sky radiometer has spectral interference
15 filters centered at selected wavelengths: 340, 380, 440, 500, 670, 870, 1020 and 1640 nm. The
16 real time operation of the data acquisition and motion steering are controlled by
17 microprocessors. Sequence of the measurements is provided automatically every clear day,
18 every 15 minutes (Holben et al., 1998). The data accuracy is 0.01 (visible solar radiation) or
19 0.02 (ultraviolet) (Smirnov et al., 2000). The AERONET provides three levels of data: level 1.0
20 (raw data), level 1.5 (cloud-screened data) and level 2.0 (quality-assured data). For the
21 detailed description see AERONET website (<http://aeronet.gsfc.nasa.gov/>).

22 The IOPAN based data obtained with a Microtops II sunphotometer were collected
23 and processed with the pre - and post - field calibration, automatic cloud clearing and were
24 manually inspected. These portable instruments made by Solar Light Company are capable of
25 measuring the total ozone column, total precipitable water vapor and aerosol optical depth
26 (Morys et al., 2001; Ichoku et al., 2002). Each of these parameters is automatically derived by
27 the instrument from equations installed by the manufacturer. The Microtops II instruments
28 currently in use at the IOPAN have five channels, but they may have one of two
29 configurations: 340, 440, 675, 870, 936 nm or 440, 500, 675, 870, and 936 nm. The estimates
30 of uncertainty of the AOD in each channel oscillates around 0.02. Detailed instrument
31 description is available at the AERONET webpage (<http://aeronet.gsfc.nasa.gov>) and has been
32 presented by Markowicz et al., (2012) and Zawadzka et al., (2014).

33 In this paper, we also used the data from Koldeway Station in Ny-Alesund performed
34 by AWIPEV. Data from 2000 until 2012 were obtained using a full-automatic sun photometer
35 type SP1A produced by Dr. Schulz and Partner GmbH. The instrument covers a spectral
36 range from 350 nm to 1050 nm in 17 channels. It automatically tracks the sun, which ensures
37 continuity of the measurements. The AOD uncertainty is 0.01 (Toledano et al., 2012).

38 39 **3. Methodology**

40
41 The AOD is a key parameter in aerosol studies which describes the entire atmospheric
42 column and is derived from the Beer-Bouguer-Lambert law. In case of Cimel and SP1A sun
43 photometers the AOD is obtained using the following algorithm. The total optical depth of the
44 atmosphere (τ) is obtained from the absolute direct signal from the ground level ($S(\lambda)$):

$$45 S(\lambda) = S_0(\lambda) \cdot e^{(-\tau m)}. \quad (1)$$

46
47
48 where: $S_0(\lambda)$ is signal at the top of the atmosphere (with earth-sun distance correction), m –
49 air mass. The AOD (τ_a) is obtained after subtraction of the Rayleigh optical depth (τ_R),
50 contribution and ozone optical depth (τ_{O_3}) for the 670 nm channel:

$$\tau_a = \tau - \tau_R - \tau_{O_3}. \quad (2)$$

The Ångström Exponent (AE) is indicative of the size predominance. From spectral AOD at channels 440, 670 and 870 nm data are calculated AE:

$$\tau_a(\lambda) = \beta(\lambda)^{-\alpha}. \quad (3)$$

The final post-processing data including sequencing, cloud-screening is carried out with the AERONET protocols (Smirnov et al., 2000).

The Microtops II calculates the AOD value at each wavelength based on the channel's signal, its extraterrestrial constant, atmospheric pressure (for Rayleigh scattering), time and location. Solar distance correction is automatically applied. All optical depth calculations are based on the Bouguer-Lambert-Beer law. The AOD formula is as follows:

$$AOT_\lambda = \frac{\ln(V_{0\lambda}) - \ln(V_\lambda \cdot SDCORR)}{m} - \tau_R \cdot \frac{P}{P_0}. \quad (4)$$

where: $\ln(V_{0\lambda})$ is the AOD calibration constant, V_λ is the signal intensity in [mV], SDCORR is the mean Earth-Sun distance correction, m is the optical air mass, τ_R is the Rayleigh optical depth, and P and P_0 are station pressure and standard sea-level pressure (1013.25 mB), respectively (Morys et al., 2001).

Typically, aerosol optical depths are derived from ground-based techniques. Sun photometer is a standard instrument which gives the integral for the total atmospheric column. This is the first step to build up the parameters which will determine the aerosol optical characteristics.

In our analyses we used Level 2.0 data. Such choice has already limited our data to those which have already been cloud-screened and quality assured. As a result we have obtained a total of 522 days and 11 387 measurements from all stations.

We present the AOD data only at a wavelength of 500 nm. We characterized the slope of these spectra characteristics by the Ångström Exponent, which is the function of the particle size distribution. It is calculated for the range 440-870 nm according to the AERONET protocol.

The presence of clouds is not always possible to detect, especially with thin Cirrus clouds or drifting snow crystals (Rozwadowska and Sobolewski, 2010). Thus the data were also manually inspected with meteorological observation (WMO, MODIS) if necessary. This strategy was also followed with the Microtops II data.

For the IOPAN measurements we adopted a similar strategy to that of the AERONET. Data were collected during the IOPAN routine, annual expeditions (AREX-Arctic Expedition) or during dedicated campaigns within the scope of the research projects, such as e.g. iAREA (<http://polandaod.pl/>). IOPAN data were recalibrated with the strategy presented in the instrument User Guide and according to the Ichoku et al. (2002). Data were recalculated based on formula 4. Then the detection of clouds was checked with the satellite and the WMO. Data with presence of cirrus clouds were rejected. From each series of 5 shots only the lowest value was used. Sequencing the data into series of five "shots" with two minutes time limit allows to improve the quality of the data after choosing the best result.

The SP1A instruments operated at the AWIPEW station are calibrated in October at Zugspitze or in February at Izana/Tenerife, Spain using the well-known Langley procedure for solar applications (Shaw, 1976). More details are available in Herber et al. (2002). Data from SP1A contain 594 days in 159273 measurements. The AWIPEW data were cleared from

1 instrument's error and a computational algorithm has been applied, in which we analyzed the
2 'suspect' data (errors, clouds, snowstorms, etc.). The 'suspect' data meet the following
3 conditions:

4 1) $AOD > 0.1$

5 In this case each AOD point which meets such criterion is classified as an event (haze,
6 pollution, clouds etc.),

7 2) $|AOD_2 - AOD_1| \geq 0.04$

8 In this case data when absolute value of the difference between successive measurements
9 during the same day is higher or equals 0.04 has been chosen. This condition filters out Arctic
10 Haze from the selected data. The expected variability of an Arctic Haze is very low during all
11 analyzed events (AOD values are stable).

12 3) $STD_{AOD} \geq 0.02$

13 Similar condition which informs about daily variability. Only the days which meet the
14 previous conditions and with standard deviation higher or equal 0.02 have been left in this
15 step.

16 After these 3 steps we were checking if the dates did not cover dates of data from other
17 instruments. Only different dates have been left. The extracted data were evaluated with
18 respect to Cloud - Aerosol Lidar and Pathfinder Satellite Observation (CALIPSO), MODIS
19 data and also with the World Meteorological data for weather station in Ny-Alesund.

20 Similar conditions were adopted for the Angstrom exponent:

21
22 1. $AE \geq -0.2$ & $AE \leq 2$

23 In this case we selected the Angstrom exponent with extreme values, which could be a
24 systematic error of instruments, especially for the SPIA for four years of measurements.

25
26 2. $|AE_2 - AE_1| \geq 2$

27 Difference between successive measurements as an absolute value during the same day higher
28 or equals 2. Chosen values are very unusual during the same day with stable values of AOD.

29
30 3. $AE_{mean} - 2AE_i \geq 2$

31 Difference between mean value of the AOD and double variable value higher than 2. This
32 condition selects outliers from the mean AE value.

33 34 **4. Results and discussion**

35
36 Looking more closely in the data we distinguished those for which AOD exceed 0.1.
37 Those data were used for the classification of events:

38
39 1) $AOD > MEAN_{AOD} + STD_{AOD}$ as an event

40 2) $AOD > MEAN_{AOD} + 4STD_{AOD}$ as an extreme event

41
42 Such analyses allowed for the specification of the occurrence of 5.27% of events in the
43 entire data set. It gives a total of 8326 out of 157847 data rows. Extreme events account for
44 2.35 % of the data (3720 cases), and most of them occurred in 2003, 2006, 2008 and 2010.

45 While AOD gives information about the aerosol loading, the AE is related to aerosol
46 size (type). The distribution of scatterplot enables to identify aerosol sources and size
47 distribution (Toledano, 2007). For that purpose we have prepared a scatter plot of AOD
48 versus AE with information of number of measurements. Aerosols can be divided into the
49 following types:

50

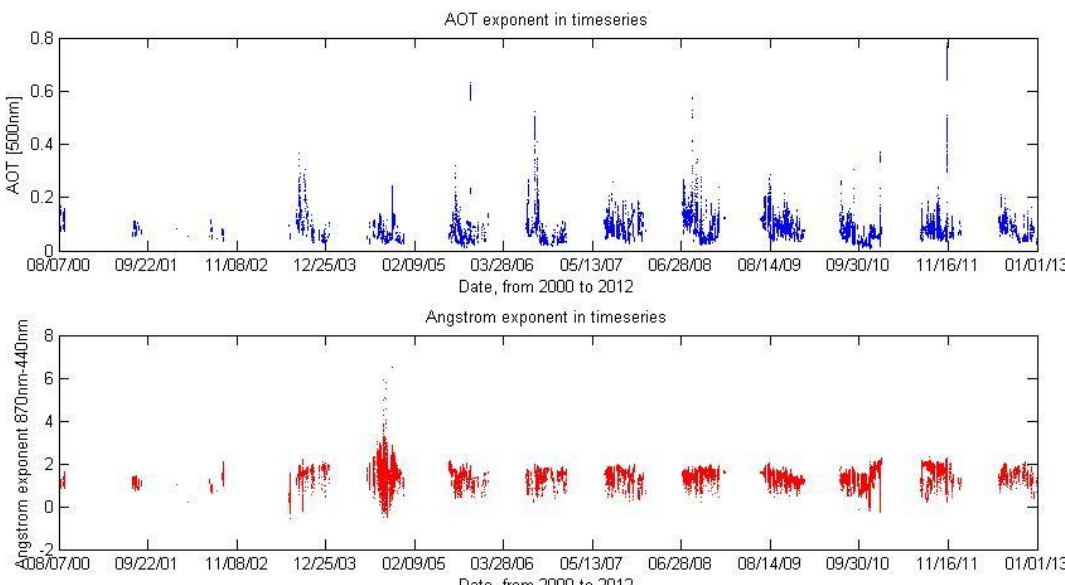
1 1. Marine aerosols
2 The pure marine should be located in the region with AOD < 0.15 and AE 0.5-1.7. This type
3 is confined to the so-called accumulation mode and is present above the oceanic areas.
4 The potential transport of continental aerosols over maritime environments interferences
5 with this type of particles, which changes density and particle size distribution.
6

7 2. Continental and biomass burning aerosols
8 Continental origin aerosols are also expected at coastal sites. This type mainly consists of fine
9 particles (<2.5 micrometers), and presents high values of AE (above 1). The AOD is very
10 variable and depends on the weather conditions (mostly around 0.15-0.30, and that
11 aerosols could be less or more polluted (AOD>2.5 during e.g. forest fires etc.). Biomass
12 burning aerosols are characterized by turbid atmosphere and large values of the AOD are
13 reported.
14

15 3. Desert Dust aerosols
16 Particles are characterized by very turbid atmosphere. Very similar values of AOD result in
17 low AE values. The AOD increase from 0.2 – 0.3 up to 1.2 against decreasing values of
18 AE from 1 to 0.
19

20 4. Mixed types of aerosols
21 Coastal and marine produce a mixed type – with typical AOD < 0.15 and AE 0.3-0.6.
22

23 In Figure 2 we present all AOD and AE data collected between 2000 and 2012 in all
24 three Spitsbergen locations, Ny-Alesund, Longyearbyen and Hornsund altogether. The data
25 have been collected in spring and summer seasons. In Figure 3 we show a scatter plot of AOD
26 (500 nm) versus AE for all data from the discussed stations.



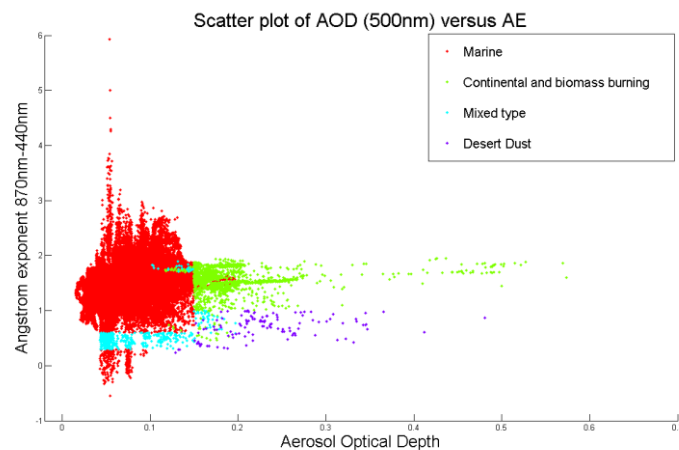
27
28 | Figure 2. AOD (500 nm) and AE for all three stations between 2000 and 2012.
29

30 The data show a natural temporal ordering which is related to seasonal changes of
31 aerosol loads into the Svalbard region. The AOD decreases from the higher events during
32 springs (mean for spring $\sim 0.085 \pm 0.046$) to more or less stable situation in summers (mean for
33 summer $\sim 0.063 \pm 0.042$). There were no events during the years 2000-2002, in these years we

1 have clear occurrence of marine aerosols. Mean for those years vary as follows: 0.084 ± 0.018 ,
2 while the Ångström exponent: 1.269 ± 0.194 .

3 Anthropogenic contamination advected with air masses from midlatitudes reach the
4 polar regions seasonally, especially in early spring and summertime. In extreme cases of such
5 advections or due to photochemical transformations of locally observed aerosols we deal with
6 the so-called Arctic Haze. Several studies have shown the occurrence of the phenomenon in
7 2005 and 2006 (Quin et al., 2007; Engval et al., 2008; Rozwadowska et al., 2010). The
8 occurrence of the strongest events during summer 2004, 2010 and spring 2006, 2008 are
9 classified as extreme events. Those high AOD values have been related to the inflow of
10 continental air masses.

11 A general overview of the data gives the information that the Aerosol Optical Depth is
12 much higher these years than a decade before. With respect to the Ångström Exponent, which
13 almost always follows the AOD values, most of its higher values should be related to the
14 anthropogenic influence. Each year the most frequent value oscillates around 1.2-1.5, but
15 between 2001 and 2011 they went up from 0.732 to 1.835.



17
18 Figure 3. Scatter plot of AOD (500 nm) versus AE for all data from the discussed stations.

19
20 The independence of Aerosol Optical Depth and Ångström exponent illustrate the
21 origin of aerosols. While AOD gives an information about the aerosol loading, the AE is
22 related to aerosol size (type), both make an interpretation of the data. This nonlinear
23 relationship between variables shows that marine is the most frequent source that can be
24 observed, presented in a form of the largest concentration on the left-side of the plot within an
25 entire spectrum of Ångström exponent and the AOD changing from 0 to 0.15. The remaining
26 part of AOD and AE spectra exceed 1, and this characterizes an anthropogenic source, such as
27 e.g. biomass burning or continental type particles. The Ångström exponent below 1 – the
28 desert dust and a mixed type, between these two sets. A statistical description of the AOD and
29 AE data is provided in Table 2 below.

30 The basic statistics, which are presented in the table were calculated for all three
31 stations. The extremes (minimum and maximum) and central tendency (mean) were used to
32 present the changing aerosol structure with years and among the different locations. The
33 variance measures how the parameters are spread out each year and almost for whole data it
34 tends to be very close to the mean (small values).

35
36
37

1 Table 2. Statistics of AOD (500 nm) and the AE with time (between 2000 and 2012)
 2 and among stations.
 3

| statio n | Nr of pts. | Year | AOD [500nm] | | | | Ångström exponent | | | |
|-------------|---------------|------|-------------|---------|-------------|----------|-------------------|---------|-------------|----------|
| | | | Minimum | Maximum | Mean ± StD | Variance | Minimum | Maximum | Mean ± StD | Variance |
| Hornsund | 853 | 2005 | 0.023 | 0.319 | 0.073±0.042 | 0.002 | 0.370 | 1.793 | 1.148±0.277 | 0.077 |
| | 923 | 2006 | 0.022 | 0.522 | 0.111±0.099 | 0.010 | 0.208 | 1.951 | 1.326±0.332 | 0.110 |
| | 1004 | 2007 | 0.037 | 0.256 | 0.089±0.032 | 0.001 | 0.300 | 1.894 | 1.269±0.387 | 0.150 |
| | 1913 | 2008 | 0.023 | 0.574 | 0.102±0.055 | 0.003 | 0.211 | 1.943 | 1.456±0.253 | 0.064 |
| | 1430 | 2009 | 0.041 | 0.285 | 0.104±0.039 | 0.002 | 0.418 | 1.806 | 1.378±0.245 | 0.060 |
| | 401 | 2010 | 0.049 | 0.305 | 0.095±0.035 | 0.001 | 0.499 | 1.877 | 1.234±0.338 | 0.115 |
| | 1534 | 2011 | 0.036 | 0.240 | 0.087±0.030 | 0.001 | 0.235 | 1.977 | 1.371±0.419 | 0.176 |
| | 1336 | 2012 | 0.025 | 0.209 | 0.082±0.032 | 0.001 | 0.391 | 2.105 | 1.561±0.271 | 0.073 |
| ye ar | 966 | 2003 | 0.029 | 0.365 | 0.095±0.060 | 0.004 | 0.447 | 2.077 | 1.609±0.261 | 0.068 |
| | 491 | 2004 | 0.024 | 0.114 | 0.048±0.013 | 0.000 | 0.491 | 1.839 | 1.357±0.251 | 0.063 |
| Ny-Alesund | 1184 | 2000 | 0.073 | 0.195 | 0.110±0.025 | 0.001 | 0.879 | 1.616 | 1.317±0.156 | 0.024 |
| | 2179 | 2001 | 0.053 | 0.110 | 0.077±0.016 | 0.000 | 0.206 | 1.432 | 1.093±0.148 | 0.022 |
| | 1233 | 2002 | 0.037 | 0.115 | 0.066±0.015 | 0.000 | 0.619 | 2.080 | 1.399±0.279 | 0.078 |
| | 888 | 2003 | 0.044 | 0.139 | 0.067±0.015 | 0.000 | -0.185 | 2.164 | 0.755±0.519 | 0.269 |
| | 10515 | 2004 | 0.027 | 0.245 | 0.088±0.046 | 0.002 | -0.192 | 2.318 | 1.609±0.485 | 0.235 |
| | 2499 | 2005 | 0.016 | 0.633 | 0.106±0.093 | 0.009 | 0.313 | 2.317 | 1.334±0.369 | 0.136 |
| | 7039 | 2006 | 0.017 | 0.264 | 0.062±0.035 | 0.001 | 0.535 | 1.802 | 1.493±0.189 | 0.036 |
| | 18442 | 2007 | 0.028 | 0.189 | 0.075±0.032 | 0.001 | 1.025 | 1.937 | 1.580±0.164 | 0.027 |
| | 16239 | 2008 | 0.025 | 0.183 | 0.078±0.038 | 0.001 | 1.046 | 1.875 | 1.536±0.153 | 0.023 |
| | 29862 | 2009 | 0.035 | 0.208 | 0.089±0.032 | 0.001 | 0.773 | 1.995 | 1.360±0.243 | 0.059 |
| | 28935 | 2010 | 0.006 | 0.126 | 0.049±0.021 | 0.000 | -0.163 | 2.237 | 1.382±0.319 | 0.102 |
| | 26021 | 2011 | 0.035 | 0.162 | 0.067±0.020 | 0.000 | 1.065 | 2.234 | 1.835±0.147 | 0.022 |

4
5
6 **5. Conclusions**
7

8 In this work we have discussed the changes of aerosol optical depth (AOD) at 500 nm
 9 and the Ångström exponent (AE) (440-870 nm) measured with use of different types of sun
 10 photometers. A general conclusion is that the results obtained over a period of 2000 and 2012
 11 show that marine source has been a dominating of aerosol sources over Spitsbergen. Some
 12 years (2005, 2006, 2008 and 2011) show very high values of AOD due to strong aerosol
 13 events such as the Arctic Haze. In general the mean AOD values increase over the period of
 14 2000 and 2012 over Spitsbergen. This may indicate the presence of larger scale of
 15 atmospheric pollution in the region. This conclusion has to be further verified by applying of
 16 chemical composition analyses.
 17

18 **6. Acknowledgements**
19

20 This research has been partly made within the framework of a Polish-Norwegian
 21 Research Programme operated by the National Centre for Research and Development under
 22 the Norwegian Financial Mechanism 2009-2014 in the frame of Project Contract No Pol-
 23 Nor/196911/38/2013., part of the Polish-Norwegian Research Programme ,partly within the
 24 scope of the GAME project and the KNOW (National Scientific Leading Centre).
 25

26 **7. References**

27 Brock C. A., Cozic J., Bahreini R., Froyd K. D., Middlebrook A. M., McComiskey A.,
 28 Brioude, J., Cooper O. R., Stohl A., Aikin K. C., de Gouw J. A., Fahey D. W., Ferrare
 29 R. A., Gao R.-S., Gore W., Holloway J. S., Hübler G., Jefferson A., Lack D. A.,
 30 Lance S., Moore R. H., Murphy D. M., Nenes A., Novelli P. C., Nowak J. B., Ogren J.
 31 A., Peischl J., Pierce R. B., Pilewskie P., Quinn P. K., Ryerson T. B., Schmidt K. S.,

- 1 Schwarz J. P., Sodemann H., Spackman J. R., Stark H., Thomson D. S., Thornberry
2 T., Veres P., Watts L. A., Warneke C., Wollny A. G., 2011: Characteristics, sources,
3 and transport of aerosols measured in spring 2008 during the aerosol, radiation, and
4 cloud processes affecting Arctic Climate (ARCPAC) Project, *Atmos. Chem. Phys.*, 11,
5 2423–2453, doi:10.5194/acp-11-2423-2011.
- 6 Dixon G. J., 1998, Laser Radars Produce Three-Dimensional Pictures, *Laser Focus World*, 4,
7 129-136.
- 8 Drollette D., 2000, Ancient Writings Come to Light, *Photonics Spectra*, 4, 40.
- 9 Dubovik O., Holben B., Eck T.F., Smirnov A., Kaufman Y.J., King M.D., Tanré D., Slutsker
10 I., 2002, Variability of absorption and optical properties of key aerosol types observed
11 in worldwide locations, *J. Atmos. Sci.* 59, 3, 590-608, DOI: 10.1175/1520-
12 0469(2002)059<0590:VOAAOP>2.0.CO;.
- 13 Engvall A.-C., Krejci R., Ström J., Treffeisen R., Scheele R., Hermansen O., Paatero J.,
14 2008, Changes in aerosol properties during spring-summer period in the Arctic
15 troposphere, *Atmos. Chem. Phys.*, 8, 445–462, [http://www.atmos-chem-](http://www.atmos-chem-phys.net/8/445/2008/)
16 [phys.net/8/445/2008/](http://www.atmos-chem-phys.net/8/445/2008/).
- 17 Fisher J. A., Jacob D. J., Purdy M. T., Kopacz M., Le Sager, P., Carouge C., Holmes C. D.,
18 Yantosca R. M., Batchelor R. L., Strong K., Diskin G. S., Fuelberg H. E., Holloway J.
19 S., Hyer E. J., McMillan W. W., Warner J., Streets D. G., Zhang Q., Wang Y., and Wu
20 S., 2010, Source attribution and interannual variability of Arctic pollution in spring
21 constrained by aircraft (ARCTAS, ARCPAC) and satellite (AIRS) observations of
22 carbon monoxide, *Atmos. Chem. Phys.*, 10, 977–996, doi:10.5194/acp-10-977-2010.
- 23 Heintzenberg J., Tuch T., Wehner B., Wiedensohler A., Wex H., Ansmann A., Mattis I.,
24 Müller D., Wendisch M., Eckhardt S., Stohl A., 2003, Arctic haze over Central
25 Europe, *Tellus Series B-Chemical and Physical Meteorology* 55 (3): 796-807
- 26 Herber A., Thomason L. W., Gernandt H., Leiterer U., Nagel D., Schulz K. H., Kaptur J.,
27 Albrecht T., Notholt J., 2002, Continuous day and night aerosol optical depth
28 observations in the Arctic between 1991 and 1999, *J. Geophys. Res.*, 107(D10), 4097,
29 doi:10.1029/2001JD000536.
- 30 Herber A., Thomason L.W., Gernandt H., Leiterer U., Nagel D., Schulz K. H., Kaptur J.,
31 Albrecht T., Notholt J., 2002, Continuous day and night aerosol optical depth
32 observations in the Arctic between 1991 and 1999. *J. Geophys. Res.*, 107 D10,
33 10.1029/2001JD000536 - AAC 6-1 to 6-14.
- 34 Holben B. N., Eck T. F., Slutsker I., Tanre D., Buis J. P., Setzer A., Vermote E., Reagan J. A.,
35 Kaufman Y. J., Nakajima T., Lavenu F., Jankowiak I., Smirnov A., 1998, AERONET
36 - a federated instrument network and data archive for aerosol characterization. *Remote*
37 *Sens. Environ.*, 66, 1–16.
- 38 Hudson S. R., 2011, Estimating the global radiative impact of the sea ice-albedo feedback in
39 the Arctic, *J. Geophys. Res.-Atmos.*, 116, D16102, doi:10.1029/2011JD015804.

- 1 Ichoku C., Levy R., Kaufman Y.J., Remer L.A., Li R., Martins V.J., Holben B.N.,
2 Abuhassan N., Slutsker I., Thomas F. Eck, Christophe Pietras, 2002, Analysis of the
3 performance characteristics of the five-channel Microtops II Sun photometer for
4 measuring aerosol optical depth and precipitable water vapor, *J. Geophys. Res.*,
5 107(D13), doi:10.1029/2001JD001302.
- 6 Labow G., 1996, Estimation of ozone with total ozone portable spectroradiometer
7 instruments. II Practical operation and comparisons, *Appl. Opt.* 35, 6084-6089.
- 8 Markowicz K. M., Flatau P. J., Kardas A. E., Remiszewska J., Stelmaszczyk K., Woeste L.,
9 2008, Ceilometer retrieval of the boundary layer vertical aerosol extinction structure,
10 *Journal of Atmospheric and Oceanic Technology*, 25 (6): 928-944.
- 11 Markowicz K. M., Zielinski T., Blindheim S., Gausa M., Jagodnicka A. K., Kardas A.,
12 Kumala W., Malinowski S. P., Petelski T., Posyniak M., Stacewicz T., 2012, Study of
13 vertical structure of aerosol optical properties with Sun photometers and ceilometer
14 during MACRON Campaign in 2007, *Acta Geophysica*, 60 (5): 1308-1337.
- 15 Mazzola M., Stone R.S., Herber A., Tomasi C., Lupi A., Vitale V., Lanconelli C., Toledano
16 C., Cachorro V.E., O'Neill N.T., Shiobara M., Aaltonen V., Stebel K., Zielinski T.,
17 Petelski T., Ortiz de Galisteo J.P., Torres B., Berjon A., Goloub P., Li Z., Blarel L.,
18 Abboudm I., Cuevas E., Stock M., Schulz K.-H., Virkkula A., 2012, Evaluation of sun
19 photometer capabilities for retrievals of aerosol optical depth at high latitudes: The
20 POLAR-AOD intercomparison campaigns, *Atmospheric Environment*, 52: 4-17 Sp.
21 Iss. SI JUN 2012,
- 22 Morys M., Mims III F.M., Hagerup S., Anderson S. E., Baker A., Kia J., and Walkup T.,
23 2001, Design, calibration, and performance of Microtops II handheld ozone monitor
24 and Sun photometer. *J. Geophys. Res.*, 106, 14,573–14,582.
- 25 Petelski T., Markuszewski P., Makuch P., Jankowski A., Rozwadowska A., 2014. Studies of
26 vertical coarse aerosol fluxes In the Bondary layer over the Baltic Sea, *Oceanologia* 56
27 (4), 2014, pp. 697-710, doi:10.5697/oc.56-4.697.
- 28 Petelski T., Piskozub J. , 2006, Vertical coarse aerosol fluxes in the atmospheric surface layer
29 over the North Polar Waters of the Atlantic, *J. Geophys. Res.*, 111, C06039,
30 doi:10.1029/2005JC003295.
- 31 Quinn P. K., Shaw G., Andrews E., Dutton E. G., Ruoho-Airola T., Gong S. L. , 2007, Arctic
32 haze: current trends and knowledge gaps, *Tellus*, 59B, 99–114.
- 33 Quinn P. K., Shaw G., Andrews E., Dutton E. G., Ruoho-Airola T., Gong S. L., 2007, Arctic
34 haze: current trends and knowledge gaps. *Tellus B*, 59(1), 99–114. doi:10.1111/j.1600-
35 0889.2006.00238.x
- 36 Rozwadowska A., Sobolewski P., 2010, Variability in aerosol optical properties at Hornsund,
37 Spitsbergen, *Oceanologia* 2010, no. 52(4), pp. 599-620 doi:10.5697/oc.52-4.599.
- 38 Rozwadowska A., Górecka I., 2012, The impact of a non-uniform land surface on the
39 radiation environment over an Arctic fjord - a study with a 3D radiative transfer model

- 1 for stratus clouds over the Hornsund fjord, Spitsbergen , *Oceanologia* 2012, no. 54(4),
2 pp. 509-543, doi:10.5697/oc.54-4.509
- 3 Rozwadowska A., Zieliński T., Petelski T., Sobolewski P., 2010, Cluster analysis of the
4 impact of air back-trajectories on aerosol optical properties at Hornsund, Spitsbergen.
5 *Atmospheric Chemistry and Physics*, 10(3), 877–893. doi:10.5194/acp-10-877-2010
- 6 Shaw G. E., 1976, Error analysis of multi-wavelength Sun photometry, *Pure Appl. Geophys.*,
7 114, 1–14.
- 8 Smimov A., Holben B.N., Eck T.F., Dubovik O., 2000, Cloud-Screening and quality control
9 algorithms for the AERONET database. *Remote Sens. Environ.* 73, 337-349.
- 10 Smirnov A., Holben B. N., Eck T. F., Dubovik O., Slutsker I., 2000, Cloud-screening and
11 quality control algorithms for the AERONET database. *Remote Sens. Environ.*, 73,
12 337–349.
- 13 Smirnov A., Holben B. N., Eck T. F., Slutsker I., Chatenet B., Pinker R. T., 2002, Diurnal
14 variability of aerosol optical depth observed at AERONET (Aerosol Robotic Network)
15 sites, *Geophys. Res. Lett.* , 29 (23), 2115, doi:10.1029/2002GL016305.
- 16 Stohl A., 2006, Characteristics of atmospheric transport into the Arctic troposphere, *J.*
17 *Geophys. Res.-Atmos.*, 111, D11306,doi:10.1029/2005jd006888.
- 18 Toledano C., Cachorro V., Gausa M., Stebel K., Aaltonen V., Berjon A., Ortis J. P., de
19 Frutos A. M., Bennouna Y., Blindheim S., Myhre C. L., Zibordi G., Wehrli C., Kratzer
20 S., Hakanson B., Carlund T., de Leuw G., Herber A., 2012, Overview of Sun
21 photometer measurements of aerosol properties in Scandinavia and Svalbard ,
22 *Atmospheric Environment.*, 52 , pp. 18-28 . doi: 10.1016/j.atmosenv.2011.10.022
- 23 Tomasi C., Vitale V., Lupi A., Di Carmine C., Campanelli M., Herber A., Treffeisen R.,
24 Stone R. S., Andrews E., Sharma S., Radionov V., von Hoyningen-Huene W., Stebel
25 K., Hansen G. H., Myhre C. L., Wehrli C., Aaltonen V., Lihavainen H., Virkkula A.,
26 Hillamo R., Stroem J., Toledano C., Cachorro V. E., Ortiz P., de Frutos A. M.,
27 Blindheim S., Frioud M., Gausa M., Zielinski T., Petelski T., Yamanouchi T., 2007,
28 Aerosols in polar regions: A historical overview based on optical depth and in situ
29 observations, *J. Geophys. Res.*, 112, D16205, doi:10.1029/2007JD008432.
- 30 Treffeisen R., Herber A., Ström J., Shiobara M., Yamanouchi T., Yamagata S., Holmén K.,
31 Kriew M., & Schrems O., 2011, Interpretation of Arctic aerosol properties using
32 cluster analysis applied to observations in the Svalbard area. *Tellus B*, 56(5).
33 doi:10.3402/tellusb.v56i5.16469.
- 34 Zawadzka O., Makuch P., Markowicz K.M., Zielinski T., Petelski T., Ulevicius V.,
35 Strzalkowska A., Rozwadowska A., Gutowska D., 2014, Studies of aerosol optical
36 depth with use of Microtops sun photometers and MODIS detectors in the coastal
37 areas of the Baltic Sea, *Acta Geophysica* , vol. 62, no. 2, Apr. 2014, pp. 400-422,
38 DOI: 10.2478/s11600-013-0182-5, 2014.

1 Zielinski T., 2004, Studies of aerosol physical properties in coastal areas. *Aerosol*
2 *Science&Technology*, 38 (5): 513-524,

3 Zielinski T., Petelski T., Makuch P., Strzalkowska A., Ponczkowska A., Markowicz K. M,
4 Chourdakis G., Georgoussis G., Kratzer S., 2012, Studies of aerosols advected to
5 coastal areas with use of remote techniques, *Acta Geophysica*, vol. 60, no. 5, DOI:
6 10.2478/s11600-011-0075-4, 1359-1385.

7